Journal of Alloys and Compounds 509 (2011) 7205–7209

Contents lists available at ScienceDirect

Journal of Alloys and Compounds

journal homepage: www.elsevier.com/locate/jallcom

Sol–gel synthesis and electrochemical performance of $Li_4Ti_5O_{12}$/graphene composite anode for lithium-ion batteries

Hongfa Xiang, Bingbing Tian, Peichao Lian, Zhong Li, Haihui Wang*

School of Chemistry & Chemical Engineering, South China University of Technology, Guangdong, Guangzhou 510640, PR China

ARTICLE INFO

Article history:
Received 12 November 2010
Received in revised form 9 April 2011
Accepted 11 April 2011
Available online 20 April 2011

Keywords:
$Li_4Ti_5O_{12}$
Graphene
Lithium-ion battery
Sol–gel
Safety

ABSTRACT

$Li_4Ti_5O_{12}$/graphene composite was prepared by a facile sol–gel method. The lattice structure and morphology of the composite were investigated by X-ray diffraction (XRD) and scanning electronic microscopy (SEM). The electrochemical performances of the electrodes have been investigated compared with the pristine $Li_4Ti_5O_{12}$ synthesized by a similar route. The $Li_4Ti_5O_{12}$/graphene composite presents a higher capacity and better cycling performance than $Li_4Ti_5O_{12}$ at the cutoff of 2.5–1.0 V, especially at high current rate. The excellent electrochemical performance of $Li_4Ti_5O_{12}$/graphene electrode could be attributed to the improvement of electronic conductivity from the graphene sheets. When discharged to 0 V, the $Li_4Ti_5O_{12}$/graphene composite exhibited a quite high capacity over 274 mAh g^{-1} below 1.0 V, which was quite beneficial for not only the high energy density but also the safety characteristic of lithium-ion batteries.

1. Introduction

Lithium-ion batteries are now not only widely used as energy storage devices for portable electronic devices, but also have been come into use for electric vehicles (EV), hybrid electric vehicles (HEV) and plug-in hybrid electric vehicles (PHEV) due to their high energy density and long lifetime. For the development of large-scale lithium-ion batteries for the vehicle applications, it is very important to improve power density and cycling performance of the state-of-the-art batteries. Comparing to widely-used graphite anode, spinel $Li_4Ti_5O_{12}$ has a very flat plateau at around 1.5 V versus Li^+/Li and displays excellent reversibility and structural stability as a zero-strain insertion material in the charge–discharge process [1]. The high voltage plateau can avoid furious reductive decomposition of carbonate solvents so that solid electrolyte interface (SEI) layer is negligible. Moreover, the operation potential at 1.5 V vs. Li^+/Li is quite gentle for some solvents or additives to be applied in the electrolyte [2,3]. So the lithium-ion batteries with $Li_4Ti_5O_{12}$ anodes are applicable in more circumstances, with important advantages in terms of cycling performance and thermal stability, although the output voltage of lithium-ion batteries with $Li_4Ti_5O_{12}$ anodes is lower than that of lithium-ion batteries with carbonaceous anodes.

The major obstacle to the practical applications of $Li_4Ti_5O_{12}$ is its intrinsically poor conductivity at room temperature ($<10^{-13}$ S cm^{-1}) [4,5]. Several methods have been utilized to improve the electronic conductivity of $Li_4Ti_5O_{12}$, such as doping with foreign metal ions [6–10], surface modification or coating with conductive carbon or metal material [11–16] and preparation of composites containing some excellent conductive components [17,18]. Among these methods, preparation of $Li_4Ti_5O_{12}$-based composites using high conductive and low-cost carbon materials by a facile route is practicable and economical for large-scale industrialization.

In recent years, graphene with superior electronic conductivity, high surface area of over 2600 m^2/g, excellent thermal properties and mechanical properties, has attracted much attention in the field of material science [19,20]. Graphene and graphene-based composites have been widely investigated in the lithium-ion batteries and other electrochemical devices [21–26]. In the composites consisting of graphene and metal oxides, graphene usually plays a vital role as a conductive component [21,22,25]. Besides its excellent conductivity, the advantage of high surface area can improve the interfacial contact with the poor-conductive particles. Recently, Zhu and his coworkers have prepared graphene-embedded $Li_4Ti_5O_{12}$ nanofibers by electrospinning deposition and got improved electrochemical performance [27]. But the preparation is very intricate and difficult to scale up. In this paper, we propose to prepare $Li_4Ti_5O_{12}$/graphene composite in a facile sol–gel method. Furthermore, the electrochemical performance of this composite is investigated by

* Corresponding author. Fax: +86 20 87110131.
E-mail address: hhwang@scut.edu.cn (H. Wang).

0925-8388/$ – see front matter © 2011 Elsevier B.V. All rights reserved.
doi:10.1016/j.jallcom.2011.04.065

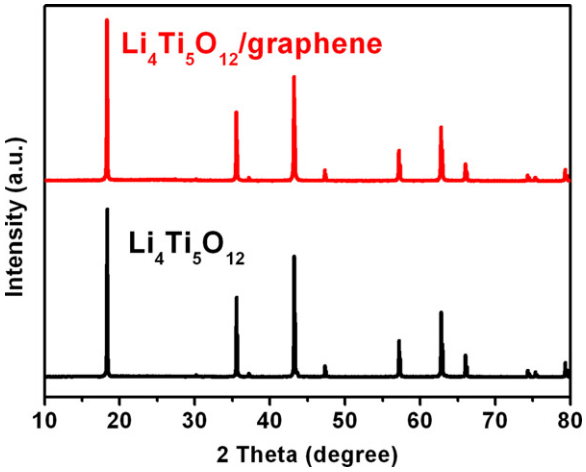

Fig. 1. XRD patterns of $Li_4Ti_5O_{12}$ and the $Li_4Ti_5O_{12}$/graphene composite prepared by the sol–gel method.

comparing with the pristine $Li_4Ti_5O_{12}$ anode in the lithium-ion batteries.

2. Experimental

2.1. Materials synthesis

$Li_4Ti_5O_{12}$/graphene composite was synthesized by a facile sol–gel method. Lithium acetate (CH_3COOLi), tetrabutyl titanate ($Ti(OC_4H_9)_4$) and graphene sheets (8 wt.% of the theoretical $Li_4Ti_5O_{12}$) were mixed in ethanol under vigorously stirring to form a sol. The molar ratio of Li and Ti was set at 4:5. The graphene sheets were prepared from graphene oxide by rapid thermal expansion at 1050 °C in nitrogen atmosphere [28]. Graphene oxide was obtained from graphite powder following the method described by Hummers [29]. After the sol was dried at 120 °C for 10 h, a gel was formed and then calcined in nitrogen atmosphere at 800 °C for 12 h to obtain the final powder. For comparison, pristine $Li_4Ti_5O_{12}$ powder was prepared in a similar way without graphene added, and the details also can be found in our previous work [6]. The final products of $Li_4Ti_5O_{12}$/graphene and $Li_4Ti_5O_{12}$ are black and light blue, respectively.

2.2. Cell assembly

The electrochemical performance of $Li_4Ti_5O_{12}$ and the $Li_4Ti_5O_{12}$/graphene composite was investigated using coin cells (CR2032). In order to make an electrode laminate, a slurry containing 82 wt.% $Li_4Ti_5O_{12}$ or $Li_4Ti_5O_{12}$/graphene and 10 wt.% Super P carbon black and 8 wt.% polyvinylidene fluoride (PVDF) dispersed in N-methyl-2-pyrrolidinone (NMP) was cast onto a copper current collector. After vacuum drying at 70 °C, the laminate was punched into discs (Φ14 mm) for assembling the cells. The mass loading in the electrode was controlled at about 1.5 mg cm^{-2}. Celgard 2400 microporous polypropylene membrane was used as separator. The electrolyte consisted of a solution of 1 M $LiPF_6$ in ethylene carbonate (EC)/diethyl carbonate (DEC) (1:1, w/w). Highly pure lithium foil was used as the counter electrode. Finally, the coin cells were assembled in an argon-filled glove box (Mikrouna, super 1220) where the oxygen and moisture contents were less than 1 ppm.

2.3. Characterization

The crystal structure of the powder was characterized on a Bruker D8 Advance X-ray diffraction using a Cu Kα radiation source (λ = 1.5406 Å). The diffraction data were collected for 2 s at each 0.02° step width over a 2θ range from 10° to 80°. The particle size and morphology were observed by scanning electron microscopy (SEM, LEO 1530 VP). The carbon content in the $Li_4Ti_5O_{12}$/graphene composite was determined by an element analyzer (Vario EL III).

The assembled cells were galvanostatically cycled at different current rates on a multi-channel battery cycler (Neware BTS2300, Shenzhen). Here all the current rates, either for the pristine $Li_4Ti_5O_{12}$ or the $Li_4Ti_5O_{12}$/graphene composite, were determined from the theoretical capacity (175 mAh g^{-1}) of $Li_4Ti_5O_{12}$. The voltage cutoffs for the discharge–charge tests were set at 2.5–1.0 V or 2.5–0 V. All the tests were performed at room temperature.

3. Results and discussion

3.1. Preparation of the $Li_4Ti_5O_{12}$/graphene composite

For all the graphene-based composites, one of the key issues is the graphene chosen for the preparation of the composites. The properties of the used graphene materials significantly depend on their synthesis methods. As we all know, graphene materials can be prepared in many ways. The most popular way is to prepare graphene oxide first and then get graphene sheets by chemical reduction or thermal reduction [30–32]. In our previous work, we prepared high quality graphene sheets with fewer layers (about 4 layers) and large specific surface area (492.5 m^2 g^{-1}) through thermal exfoliation of graphene oxide [28]. The initial reversible

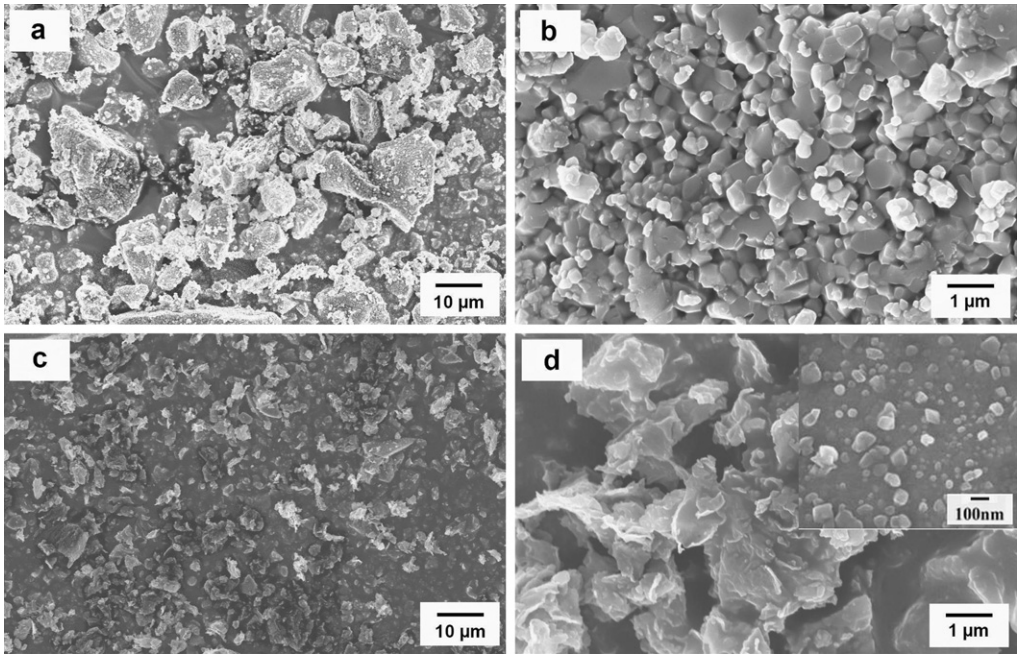

Fig. 2. SEM images of $Li_4Ti_5O_{12}$ (a and b) and the $Li_4Ti_5O_{12}$/graphene composite (c and d).

specific capacity was as high as 1264 mAh g^{-1} at a current density of 100 mA g^{-1}. The capacity still kept 848 mAh g^{-1} after 40 cycles. Recently, these graphene sheets have been used to successfully prepare the Fe_3O_4/graphene composite. Owing to fewer layers and higher surface area of as-prepared graphene sheets, it is more facile to disperse them in the ethanol solution and form a homogeneous sol. Herein, we use this kind of graphene to prepare the $Li_4Ti_5O_{12}$/graphene composite.

X-ray diffraction (XRD) patterns of the $Li_4Ti_5O_{12}$ and the $Li_4Ti_5O_{12}$/graphene composite are shown in Fig. 1. The diffraction peaks of the two samples are similar and conform to JCPDS card No.49-0207 in accordance with the spinel $Li_4Ti_5O_{12}$ standard, indicating that both represent a single-phase cubic structure with *Fd3m* space group. There is no any other impurity phase detected. Usually graphene is apt to stack into multilayers and form a graphitic structure. Here $Li_4Ti_5O_{12}$ particles prohibit the stack by jamming the graphene sheets, and thus no any diffraction according to graphitic structure was detected. Moreover, graphene in the composite is in amorphous form. In addition, the result obtained from the element analyzer indicates that the amount of carbon in the $Li_4Ti_5O_{12}$/graphene is about 7.8 wt.%, which is basically in agreement with the content of the graphene sheets added into the synthetic system.

Fig. 2 shows the SEM images of $Li_4Ti_5O_{12}$ and the $Li_4Ti_5O_{12}$/graphene composite powders. From Fig. 2a and b, it is clear that the size of the obtained $Li_4Ti_5O_{12}$ powder is about 5–10 μm, and the primary particles is in the size of 200–800 nm. However, the $Li_4Ti_5O_{12}$/graphene composite with the size of 1–5 μm is composed of the graphene sheets and $Li_4Ti_5O_{12}$ particles less than 100 nm (Fig. 2c and d). It seems that the introduction of graphene sheets in the sol–gel process is helpful to suppress the aggregation of $Li_4Ti_5O_{12}$ particles under high temperature, possibly because of the partition effect of the graphene sheets. The smaller size of the $Li_4Ti_5O_{12}$ particles means the shorter diffusion distance for lithium ions. So the $Li_4Ti_5O_{12}$/graphene composite should be a promising anode material with excellent cell performances. Additionally, almost all the $Li_4Ti_5O_{12}$ particles are anchored on the surface of the highly conductive graphene sheets. Even though the oxygen-containing groups on the graphene sheets has been remarkably reduced after the heat treatment at the high temperature (1050 °C), there are still plenty of the polar groups left, which interact strongly with the metal ions in the sol. The interaction is helpful to anchor the $Li_4Ti_5O_{12}$ particles on the graphene sheets. Additionally lots of cavities in the graphene sheets can accommodate the $Li_4Ti_5O_{12}$ particles. As a result, the homogeneous and stable $Li_4Ti_5O_{12}$/graphene composite has been prepared successfully, as shown in Fig. 2c and d.

3.2. Electrochemical performance

The electrochemical performance of the $Li_4Ti_5O_{12}$/graphene composite was investigated by comparing with the pristine $Li_4Ti_5O_{12}$. Fig. 3 shows the initial discharge–charge curves of the cells with the electrodes using $Li_4Ti_5O_{12}$ and the $Li_4Ti_5O_{12}$/graphene composite at 0.2 C and 10 C between 1.0 and 2.5 V. From Fig. 3a, $Li_4Ti_5O_{12}$ exhibits a quite high reversible capacity of 165 mAh g^{-1} with the coulombic efficiency of 94% at 0.2 C. However, for the $Li_4Ti_5O_{12}$/graphene composite, the reversible capacity and coulombic efficiency are 174 mAh g^{-1} and 99%, respectively. Above all, it is distinctively shown that the gap between the charge voltage plateau and the discharge voltage plateau for the $Li_4Ti_5O_{12}$/graphene composite is quite small, compared with the pristine $Li_4Ti_5O_{12}$. The smaller voltage drop as well as the higher capacity could be attributed to the enhanced conductivity from the introduction of graphene. As shown in Fig. 3b, the

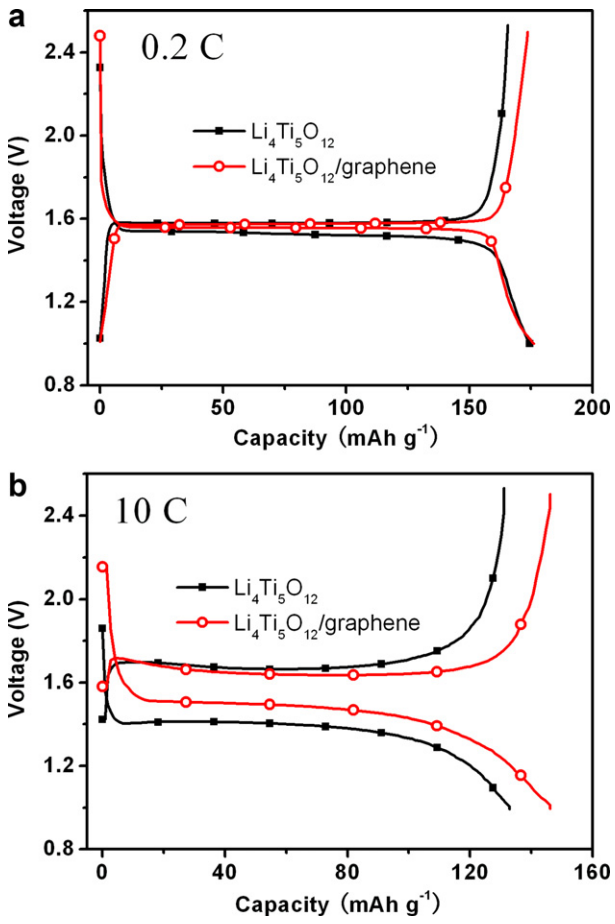

Fig. 3. The initial discharge–charge curves of the cells with the electrodes using $Li_4Ti_5O_{12}$ and the $Li_4Ti_5O_{12}$/graphene composite at 0.2 C (a) and 10 C (b) between 1.0 and 2.5 V.

difference between $Li_4Ti_5O_{12}$ and the $Li_4Ti_5O_{12}$/graphene composite at 10 C becomes more obvious than that at 0.2 C (Fig. 3a). At 10 C, the reversible capacity of the $Li_4Ti_5O_{12}$/graphene composite is about 146 mAh g^{-1}, which is much higher than that of $Li_4Ti_5O_{12}$ (131 mAh g^{-1}). The discharge plateau of the former is about 1.5 V, but the latter has only a discharge plateau of 1.4 V. The significant difference between $Li_4Ti_5O_{12}$ and its composite demonstrates that graphene in the $Li_4Ti_5O_{12}$/graphene composite remarkably improves the reversible capacity of $Li_4Ti_5O_{12}$, especially at the higher current rate.

The cycling stability of the cells with the electrodes using $Li_4Ti_5O_{12}$ and the $Li_4Ti_5O_{12}$/graphene composite at 0.2 C and 10 C are investigated, as shown in Fig. 4. At 0.2 C, the discharge capacity of the $Li_4Ti_5O_{12}$/graphene is slightly higher than the capacity of the $Li_4Ti_5O_{12}$ and the specific capacity retention during 100 cycles is 94%. At 10 C, the 100th discharge capacity of the $Li_4Ti_5O_{12}$/graphene is 110 mAh g^{-1}, which is much higher than that of the $Li_4Ti_5O_{12}$ (84 mAh g^{-1}). The improvement in capacity retention especially in high rate capacity can be attributed to the introduction of superior conductive graphene. On the one hand, the graphene sheets induce the formation of fine $Li_4Ti_5O_{12}$ nanoparticles in the sol–gel synthesis. The reduced size means the shortened diffusion distance for lithium ions and thus the kinetics of lithium insertion/extraction is accelerated. On the other hand, the electronic conductivity of the $Li_4Ti_5O_{12}$ nanoparticles anchored to the graphene sheets is significantly improved.

Recently, Amine and his co-workers reported that a new phase generated after the spinel/rock-salt phase transition of $Li_4Ti_5O_{12}$

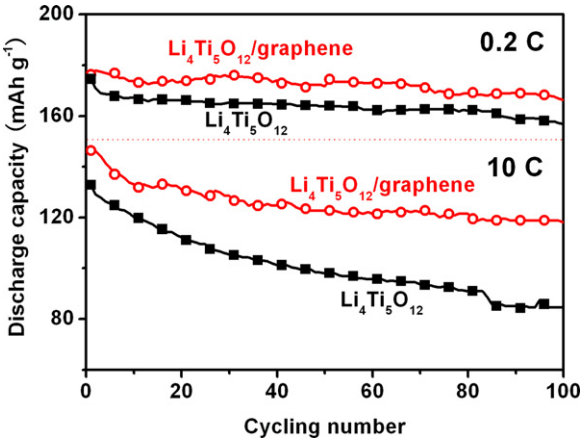

Fig. 4. Cycling performance of the cells with the electrodes using $Li_4Ti_5O_{12}$ and the $Li_4Ti_5O_{12}$/graphene composite at 0.2 C and 10 C between 1.0 and 2.5 V.

with extra lithium insertion [33]. Our recent work also indicated that the extra capacity of the $Li_4Ti_5O_{12}$ anode below 1.0 V functions to postpone overcharge and withstand high voltage in a full cell, e.g. $LiNi_{0.5}Mn_{1.5}O_4/Li_4Ti_5O_{12}$ [34]. Now we propose that the $Li_4Ti_5O_{12}$/graphene composite could provide higher capacity than the pristine $Li_4Ti_5O_{12}$ in the low voltage range (<1.0 V) from the graphene sheets. Fig. 5 shows the initial voltage profiles of the cells with the electrodes using $Li_4Ti_5O_{12}$ and the $Li_4Ti_5O_{12}$/graphene composite when discharging and charging between 2.5 and 0 V. For the pristine $Li_4Ti_5O_{12}$ definitely the discharge curve can be separated into two sections, 2.5–1.0 V region and 1.0–0 V region, with the total specific capacity of 270 mAh g^{-1}, which is close to the results of Ge's and Borghols's works [35,36]. In the first section, the capacity of about 160 mAh g^{-1} is corresponding to the transition from the spinel ($Li_4Ti_5O_{12}$) to the rock-salt structure ($Li_7Ti_5O_{12}$). However, in the following section (1.0–0 V), the discharge capacity is over 110 mAh g^{-1}, which is higher than the theoretic capacity for the single phase transition from $Li_7Ti_5O_{12}$ to $Li_{8.5}Ti_5O_{12}$ (about 87.5 mAh g^{-1}) based on the mass of the original $Li_4Ti_5O_{12}$. The extra capacity is mainly attributed to the lithium storage in the conductive carbon black and to the side reaction between the electrolyte and the electrode [2]. In our previous investigation, we proposed that the capacity of this section (below 1.0 V) was helpful to postpone the overcharge distort and thus improve the safety characteristic of the full cells [34]. So the higher capacity below 1.0 V is more advantageous for the safety of the relative lithium-ion

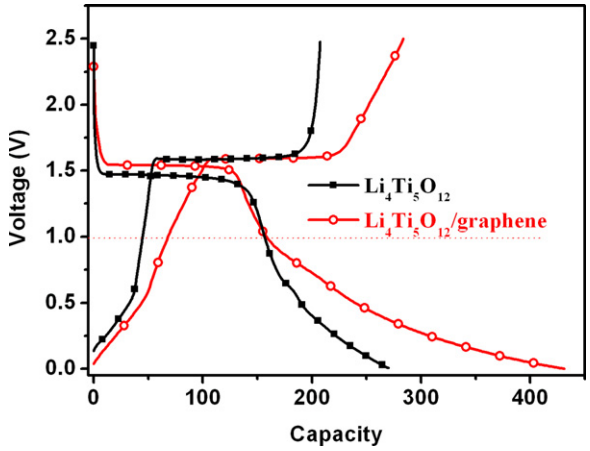

Fig. 5. The initial discharge–charge curves of the cells with the electrodes using $Li_4Ti_5O_{12}$ and the $Li_4Ti_5O_{12}$/graphene composite between 0 and 2.5 V. The current density for charge and discharge is set at 170 mA g^{-1}.

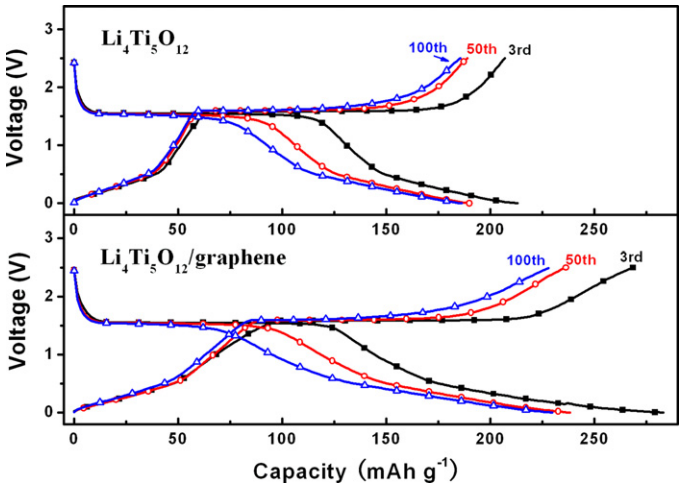

Fig. 6. The 3rd, 50th and 100th voltage profiles of the cells with the electrodes using $Li_4Ti_5O_{12}$ and the $Li_4Ti_5O_{12}$/graphene composite between 0 and 2.5 V. The current density for charge and discharge is set at 170 mA g^{-1}.

batteries. For the $Li_4Ti_5O_{12}$/graphene composite, the discharge curve is similar as that for $Li_4Ti_5O_{12}$. In the region above 1.0 V, the discharge capacity is nearly equal to that of the pristine $Li_4Ti_5O_{12}$. However, in the region below 1.0 V, the discharge capacity of 270 mAh g^{-1} is much higher than that of $Li_4Ti_5O_{12}$ (110 mAh g^{-1}). Comparing with the voltage profiles of pure graphene anode in our previous work [28], we conclude that the difference of the discharge capacity between $Li_4Ti_5O_{12}$/graphene composite and $Li_4Ti_5O_{12}$ below 1.0 V is mainly due to the lithium storage in the graphene sheets. During the charging process, the sloping lines in the regions of 0.5–1.5 V and 1.6–2.5 V correspond to total charge capacity of 125 mAh g^{-1}, which is obviously different from nearly vertical lines in the same regions for the pristine $Li_4Ti_5O_{12}$. The sloping charging curve is also the main character of graphene during charging, based on the previous literatures [28,30,31]. In addition, it is also obvious that the smaller voltage drop from the voltage gap between the charging plateau and the discharging plateau is also attributed to the introduction of highly conductive graphene. Compared with the cells cycled between 2.5 and 1.0 V, both the cells have the reduced coulombic efficiencies in the region of 2.5–0 V, 76.9% for $Li_4Ti_5O_{12}$ and 65.8% for the $Li_4Ti_5O_{12}$/graphene composite. The main reason for the reduced coulombic efficiency is possibly the irreversibly reductive decomposition of the solvents at the low potential (<1 V vs. Li^+/Li) [2,34]. Especially, for the $Li_4Ti_5O_{12}$/graphene composite, more side reactions on the active graphene sheets with high specific surface area lead to low coulombic efficiency (65.8%), which is also common in the pure graphene anode [28,30].

The 3rd, 50th and 100th voltage profiles of the cells with the electrodes using $Li_4Ti_5O_{12}$ and the $Li_4Ti_5O_{12}$/graphene composite cycled between 2.5 and 0 V are shown in Fig. 6. It is clear that the coulombic efficiencies keep at a high level above 95%, not like the initial cycle. The 3rd, 50th and 100th reversible capacities of $Li_4Ti_5O_{12}$ are 206, 189 and 185 mAh g^{-1}, respectively. The $Li_4Ti_5O_{12}$/graphene composite exhibits higher reversible capacities of 269 (3rd), 236 (50th) and 228 mAh g^{-1} (100th). Both $Li_4Ti_5O_{12}$ and the $Li_4Ti_5O_{12}$/graphene composite have visible capacity fading in the first 50 cycles and good cyclability in the next 50 cycles. Overall, it can be concluded that both $Li_4Ti_5O_{12}$ and the $Li_4Ti_5O_{12}$/graphene composite cycled in the region of 2.5–0 V have good cycling performance. It is worth noting that the capacity of the discharge plateau at ~1.5 V is decreasing even though the total discharge capacity keeps stable with the cycle number increasing. The reason for this interesting phenomenon should be a subject of further study. In brief, the $Li_4Ti_5O_{12}$/graphene composite can release

much higher capacity than $Li_4Ti_5O_{12}$, especially in the region of 1.0–0 V, which is quite beneficial for not only the high energy density but also the safety characteristic of relative lithium-ion batteries.

4. Conclusions

The $Li_4Ti_5O_{12}$/graphene composite has been prepared by a facile sol–gel process. There is no impurity phase detected but pure $Li_4Ti_5O_{12}$ cubic phase with *Fd3m* space group in the composite. SEM results indicate that homogeneous composite powders are composed of graphene sheets and fine $Li_4Ti_5O_{12}$ nanoparticles. We have demonstrated that the $Li_4Ti_5O_{12}$/graphene composite has higher capacity, especially at high current rate, and better cycling performance than the pristine $Li_4Ti_5O_{12}$. Above all, when discharged to 0 V, the $Li_4Ti_5O_{12}$/graphene composite exhibits a quite high capacity of 430 mAh g^{-1}. The higher capacity than $Li_4Ti_5O_{12}$, especially in the region of 1.0–0 V, is quite beneficial for not only the high energy density but also the safety characteristic of relative lithium-ion batteries. All the results suggest that the $Li_4Ti_5O_{12}$/graphene composite is a promising anode material for the high-energy and highly safe lithium-ion batteries.

Acknowledgements

This work was supported by National Science Foundation of China (grant no. 21006033), Program for New Century Excellent Talents in Chinese Ministry of Education (No. NECT-07-0307) and the Fundamental Research Funds for the Central Universities, SCUT (2009220038).

References

[1] T. Ohzuku, A. Ueda, N. Yamamoto, J. Electrochem. Soc. 142 (1995) 1431.
[2] X.L. Yao, S. Xie, C.H. Chen, Q.S. Wang, J.H. Sun, Y.L. Li, S.X. Lu, Electrochim. Acta 50 (2005) 4076.
[3] H.F. Xiang, Q.Y. Jin, R. Wang, C.H. Chen, X.W. Ge, J. Power Sources 179 (2008) 351.
[4] L. Cheng, X.L. Li, H.J. Liu, H.M. Xiong, P.W. Zhang, Y.Y. Xia, J. Electrochem. Soc. 154 (2007) A692.
[5] J.J. Huang, Z.Y. Jiang, Electrochim. Acta 53 (2008) 7756.
[6] B.B. Tian, H.F. Xiang, L. Zhang, Z. Li, H.H. Wang, Electrochim. Acta 55 (2010) 5453.
[7] K. Mukai, K. Ariyoshi, T. Ohzuku, J. Power Sources 146 (2005) 213.
[8] S.H. Huang, Z.Y. Wen, X.J. Zhu, Z.X. Lin, J. Power Sources 165 (2007) 408.
[9] H.L. Zhao, Y. Li, Z.M. Zhu, J. Lin, Z.H. Tian, R.L. Wang, Electrochim. Acta 53 (2008) 7079.
[10] J. Wolfenstine, J.L. Allen, J. Power Sources 180 (2008) 582.
[11] L.X. Yang, L.J. Gao, J. Alloys Compd. 485 (2009) 93.
[12] X.B. Hu, Z.J. Lin, K.R. Yang, Z.H. Deng, J.S. Suo, J. Alloys Compd. 506 (2010) 160.
[13] G.J. Wang, J. Gao, L.J. Fu, N.H. Zhao, Y.P. Wu, T. Takamura, J. Power Sources 174 (2007) 1109.
[14] J. Gao, J.R. Ying, C.Y. Jiang, C.R. Wan, J. Power Sources 166 (2007) 255.
[15] S.H. Huang, Z.Y. Wen, X.J. Zhu, Z.H. Gu, Electrochem. Commun. 6 (2004) 1093.
[16] S.H. Huang, Z.Y. Wen, B. Lin, J.D. Han, X.G. Xu, J. Alloys Compd. 457 (2008) 400.
[17] R. Cai, X. Yu, X.Q. Liu, Z.P. Shao, J. Power Sources 195 (2010) 8244.
[18] X. Li, M.Z. Qu, Y.J. Huai, Z.L. Yu, Electrochim. Acta 55 (2010) 2978.
[19] A.K. Geim, K.S. Novoselov, Nat. Mater. 6 (2007) 183.
[20] D.A. Dikin, S. Stankovich, E.J. Zimney, R.D. Piner, G.H.B. Dommett, G. Evmnenko, S.T. Nguyen, R.S. Ruoff, Nature 448 (2007) 457.
[21] S.M. Paek, E. Yoo, I. Honma, Nano Lett. 9 (2009) 72.
[22] D. Wang, D. Choi, J. Li, Z. Yang, Z. Nie, R. Kou, D. Hu, C. Wang, L.V. Saraf, J. Zhang, I.A. Aksay, J. Liu, ACS Nano 3 (2009) 907.
[23] J. Yao, X. Shen, B. Wang, H. Liu, G. Wang, Electrochem. Commun. 11 (2009) 1849.
[24] S.L. Chou, J.Z. Wang, M. Choucair, H.K. Liu, J.A. Stride, S.X. Dou, Electrochem. Commun. 12 (2010) 303.
[25] Z.S. Wu, W. Ren, L. Wen, L. Gao, J. Zhao, Z. Chen, G. Zhou, F. Li, H.M. Cheng, ACS Nano 4 (2010) 3187.
[26] K. Zhang, L.L. Zhang, X.S. Zhao, J.S. Wu, Chem. Mater. 22 (2010) 1392.
[27] N. Zhu, W. Liu, M.Q. Xue, Z. Xie, D. Zhao, M.N. Zhang, J.T. Chen, T.B. Cao, Electrochim. Acta 55 (2010) 5813.
[28] P.C. Lian, X.F. Zhu, S.Z. Liang, Z. Li, W.S. Yang, H.H. Wang, Electrochim. Acta 55 (2010) 3909.
[29] W.S. Hummers, R.E. Offeman, J. Am. Chem. Soc. 80 (1958) 1339.
[30] E. Yoo, J. Kim, E. Hosono, H. Zhou, T. Kudo, I. Honma, Nano Lett. 8 (2008) 2277.
[31] G.X. Wang, X.P. Shen, J. Yao, J. Park, Carbon 47 (2009) 2049.
[32] D. Li, M. Müller, B.S. Gilje, R.B. Kaner, G.G. Wallace, Nat. Nanotechnol. 3 (2008) 101.
[33] W. Lu, I. Belharouak, J. Liu, K. Amine, J. Electrochem. Soc. 154 (2007) A114.
[34] H.F. Xiang, X. Zhang, Q.Y. Jin, C.P. Zhang, C.H. Chen, X.W. Ge, J. Power Sources 183 (2008) 355.
[35] H. Ge, N. Li, D.Y. Li, C.S. Dai, D.L. Wang, J. Phys. Chem. C 113 (2009) 6324.
[36] W.J.H. Borghols, M. Wagemaker, U. Lafont, E.M. Kelder, F.M. Mulder, J. Am. Chem. Soc. 131 (2009) 17786.